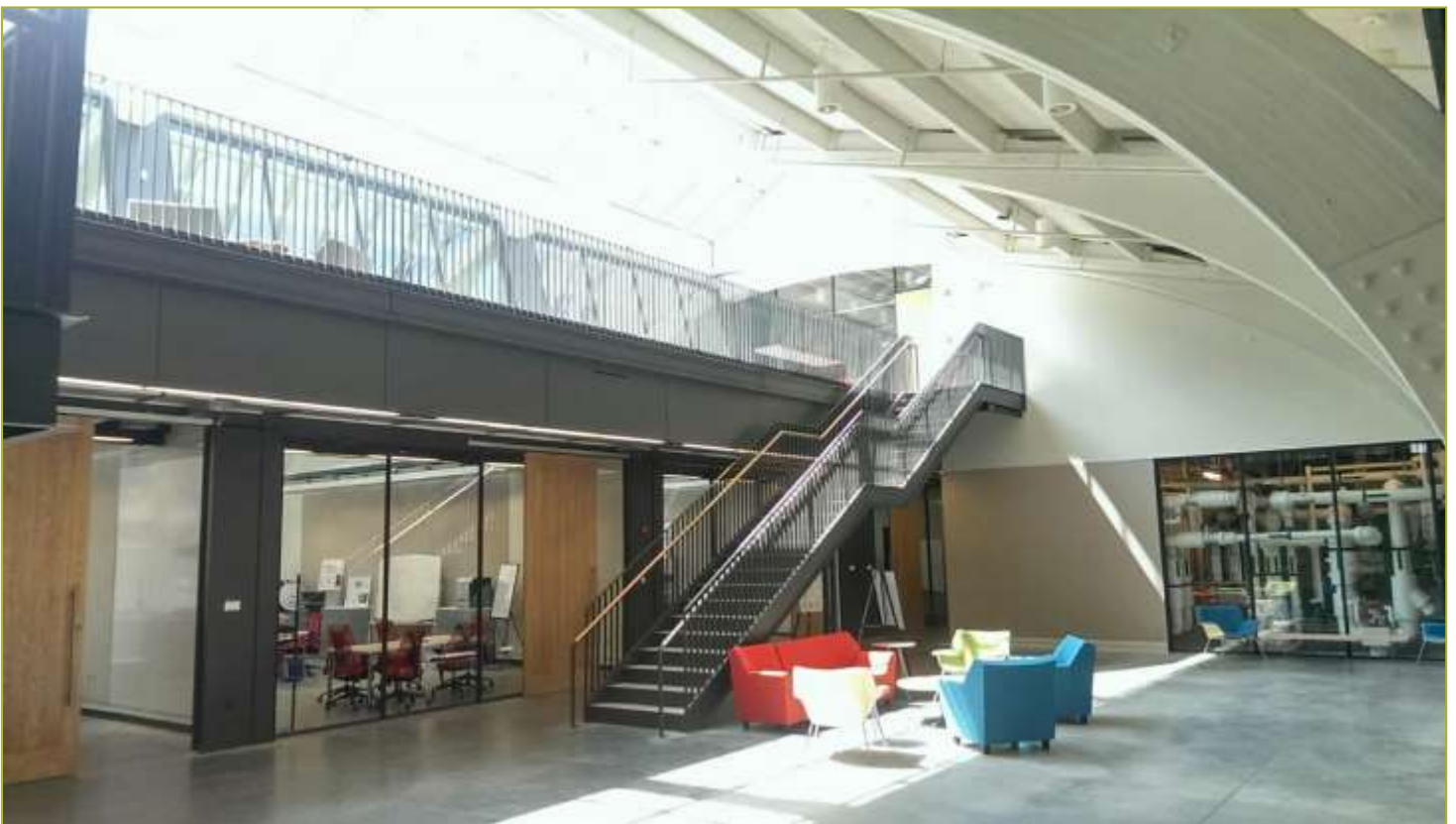# REPORT

Title: Field testing of diagnostics for state-of-the-art RTUs

Report Date: April 30, 2016

Report Author: Mikhail Gorbounov, Jinliang Wang, Murat Yasar, Hayden Reeve

CBEI REPORT

Report Abstract

Project Objectives:

- Evaluate and test cost-effective virtual sensor based RTU diagnostics with a focus on overall performance degradation (COP, capacity).

- Perform demonstrations of the FDD and fault impact methods at field sites associated with a National Account customer that has an interest in FDD for RTUs at their stores (UTRC).

- Apply developed methodology and demonstrate implementation within VOLTTRON in the laboratory including on-line estimation of the impacts of faults on performance and operating costs to determine when service should be performed (Purdue).

Major findings/Result:

- Installed required instrumentation and remote monitoring system at two field sites
- Developed, calibrated and validated referenced models for AFDD
- Demonstrated performance degradation caused by different injected faults
- Developed online field data retrieving and system operation monitoring method
- Demonstrated online AFDD through WebCTRL platform and DMS middleware
- Achieved 90% confidence on 10% performance degradation detections with no false alarm during up to 3-month monitoring periods
- Performed economic assessment of AFFD solution

Contact Information for lead researcher

Name: Mikhail Gorbounov
Institution: UTRC
Email address: gorboumb@utrc.utc.com
Phone number: 860 610 2117

Contributors

Mikhail Gorbounov, Jinliang Wang, Murat Yasar, Hayden Reeve

Contains no technical data subject to the EAR or the ITAR

CONTENTS

1 Introduction

This BP5 project builds on the BP4 evaluation and testing of RTU diagnostics with a focus on overall performance degradation [1]. The automated fault detection and diagnostics (AFDD) algorithms have been developed to be deployed within new RTUs at the factory and are based on virtual sensors developed by Purdue and fully documented in the literature [2], [3]. The faults being considered are: high or low refrigerant charge, compressor internal leakage, liquid line restriction, TXV malfunction, condenser fouling, and evaporator fouling. These faults have been identified in previous work as either occurring frequently or having a large impact [4]. The initial product offerings may, however, focus on overall degradation detection and overall fault impact on RTU performance (COP, capacity).

Recent work sponsored by the California Energy Commission [5], [6] has demonstrated that existing AFDD methods that are based on generic rules do not work well. It is now clear that AFDD needs to be engineered for specific units and should be embedded within the factory in order to achieve acceptable performance. This project is focused on developing and demonstrating scalable approaches for engineering and deploying cost-effective embedded AFDD.

UTRC has performed demonstrations of the AFDD and fault impact methods at field sites associated with a National Account customer that has an interest in AFDD for RTUs at their stores. By gathering real-world operating performance through field testing on state-of-the-art RTU systems, the goal of this project is to define and quantify the value of the diagnostics as well as determine the value and prioritization of specific faults observed in the field. UTRC will also analyze the applicability of the technology to older standard RTUs. The project will also verify the robustness of the algorithms and gather data on the frequency and severity of faults experienced in normal operation. This project will attempt to obtain reliable data on the prevalence and severity of faults in the field, installed cost, accuracy of diagnostics and false alarm rates.

2 Field Testing Preparation & Commission

2.1 Site Selection

In coordination with Carrier and ALC, UTRC selected two 7-Eleven stores in Cape Coral, Florida as the field demonstration sites. These sites were chosen because the south Florida climate is hot and humid with the RTUs operating most of the year and both sites have the same Carrier advanced WeatherMaster 50HCQ series high efficiency heat pump RTUs.

Figures 2.1 and 2.2 show both store exterior/interior views and RTUs located on the building roofs. Both stores have a 7.5 ton cooling capacity RTU providing store open space cooling and a 5 ton RTU to cool the store office space. Figure 2.3 shows the HVAC layout on the store roofs and the air duct arrangement in the stores. The HVAC configurations are very similar.

a)   50HCQA06D2M5(5 ton)   b)50HCQD08D2M5(7.5 ton)

c)   Store Exterior View   d) Store Interior View

Figure 2.1 RTUs and 7-Eleven Store (801 Cape Coral pkwy, Cape Coral, FL)

b)   50HCQA06D2M5(5 ton)   b)50HCQD08D2M5(7.5 ton)

d)   Store Exterior View   d) Store Interior View

Figure 2.2 RTUs and 7-Eleven Store (1548 Andalusia Blvd, Cape Coral, FL)

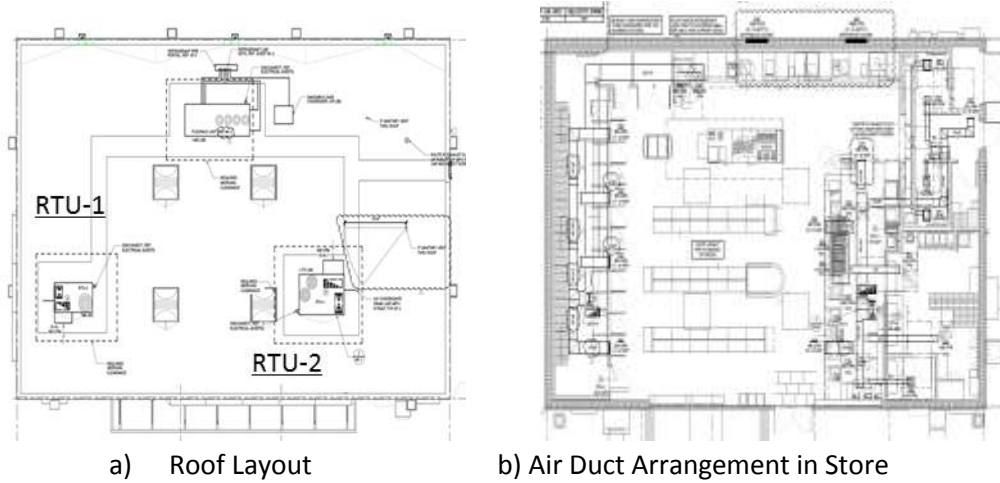| a) Roof Layout | b) Air Duct Arrangement in Store |

Figure 2.3 HVAC Layouts in 7-Eleven Stores

2.2 Instrumentation & DAQ System

Table 2.1 RTU Measurement Summary

a) RTU sensors b) Additional Sensors for AFFD

Available RTU Sensors
RA TEMP
SA TEMP
MA TEMP
OA TEMP
OA HUMIDITY/ENTHALPY
LOW REFRIGERANT PRESSURE
HIGH REFRIGERANT PRESSURE
UNIT CURRENT
SPACE TEMP
SPACE HUMIDITY
SPACE CO2

Additional RTU Sensors	Tsuc	Tdis	Tcond out	Ttxv in	Tcond air out	RH MA	RH SA
Capacity	x	x	x				
Comp. COP	x	x					
Cond. Fouling					x		
Evap. Filter blockage						x	x
Restriction in the line				x			
Refrigerant charge	x		x				
Compressor leakage	x	x					
Mass flow rate (map)	x	x					
Mass flow rate (balance)	x	x					
Reference Model						x	
Summary	x	x	x	x	x	x	x
							per circuit
							per unit

Based on Carrier's HCQ series RTU product and installation documents, a detailed measurement plan was developed. The existing and additional required sensors for RTU performance degradation detection and fault diagnostics are identified and summarized in Table 2.1. Table 2.1 (a) lists the sensors that are available already. Table 2.1 (b) shows five additional temperature sensors and two additional air humidity sensors required for the RTU AFDD. An additional temperature sensor is added to improve the air temperature measurement at the condenser outlet. Figure 2.4 shows additional temperature and humidity sensor locations along the air flow and refrigerant flow paths. In order to trend and record signals of the added sensors, a WebCRTL network accessing board (ALC I/O Flex 8160 expander), a 24 volt DC power supply and an enclosure are added to the data acquisition (DAQ) system.
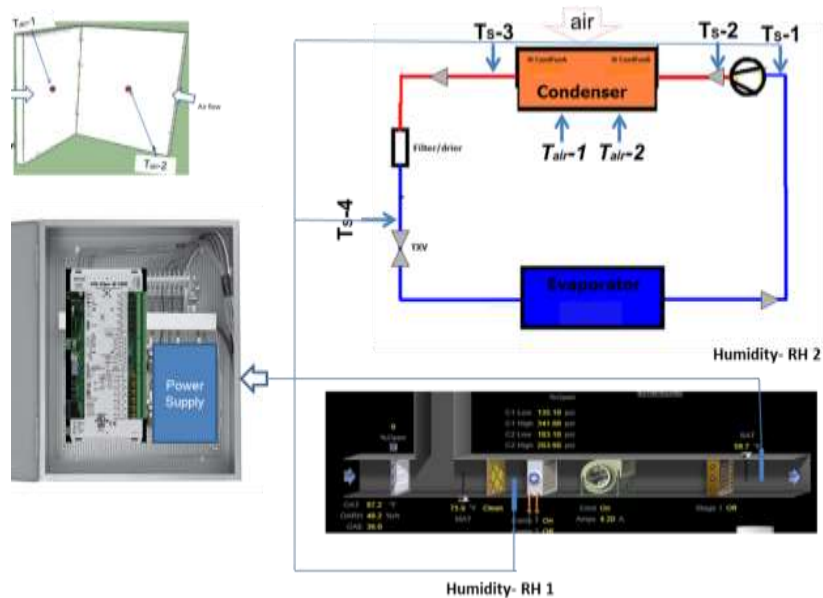
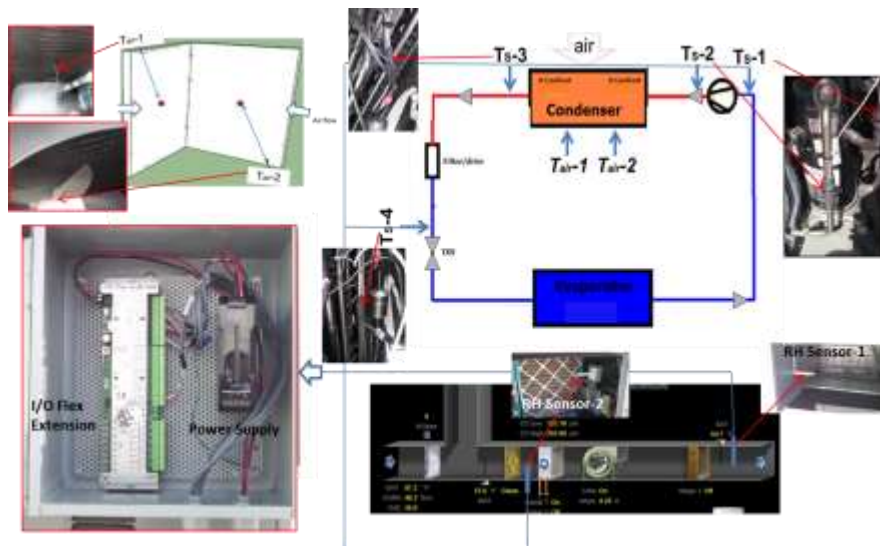Figure 2.4 Schematic of additional sensor installation

Figure 2.5 Overall Connection Layout of Installation

Six 10K type 2 thermistors and two air humidity sensors are added to each RTU unit in order to perform RTU performance degradation detection and diagnostics. Among two independent refrigerant circuits of the 7.5 Ton RTUs, only primary circuits are instrumented. Figure 2.5 shows overall connection layout of installation for each RTU. Four surface mounted thermistors (Ts-1,2,3,4) are attached to the compressor inlet and outlet, the condenser outlet and TXV inlet. Two thermistor probes are added to the condenser coil air outlet. First humidity sensor is installed inside the RTU supply air duct and second air humidity

sensor between the evaporator coil and mixing air filter. Both thermistors and humidity sensors are connected to an I/O Flex EX8160 expander card which is powered by a 24V Omtron power supply and connected to the RTU original data communication I/O flex 6126 board. Both the power supply and I/O Flex Ex 8160 expander are mounted inside an enclosure box. Figures 2.6-2.9 show overall views and installation details of all four RTUs. Figures 2.6(a)-2.9(a) highlight the enclosure box locations and RTU exterior views after installation. As highlighted in Figures 2.6(c)- 2.9(c), four 10 K Type 2 Omega surface-mount thermistors are wrapped with thermal insulation materials after their attachment. Figures 2.6(d)-2.6(d) marked the locations of two 10K Type 2 thermistor probes and two humidity probes for measuring air temperature at the condenser outlet and relative humidity at the evaporator inlet/outlet respectively.
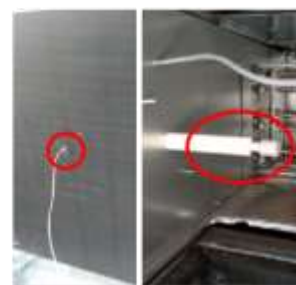

a) Exterior Photo/Enclosure
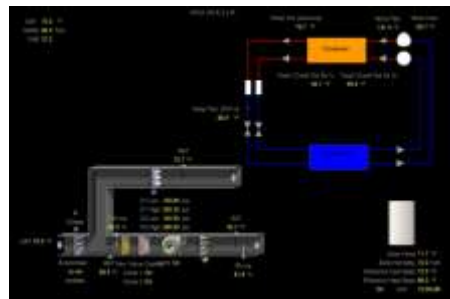
b) WebCTRL Interface

c) Thermistors along Refrigerant Loop
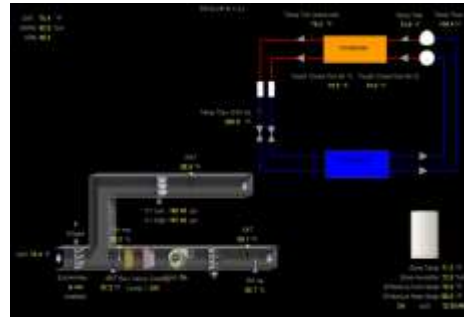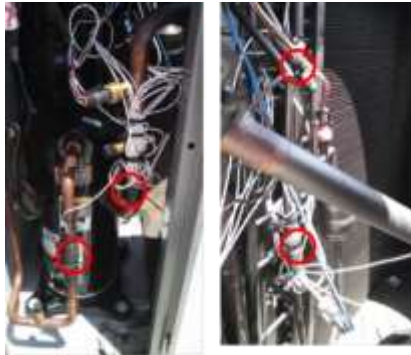

d) Air Temp Probes & RH sensors

Figure 2.6 RTU-1 at 7-Eleven Store (801 Cape Coral pkwy, Cape Coral, FL)

After the installation, all additional sensors have been mapped out and programmed in WebCTRL with the support of ALC. Figures 2.6(b)-2.9(b) show the updated WebCRTL interfaces for each RTU. The previously existing and additional sensors listed in Table 2.1 are trended in WebCRTL. The recorded data are retrieved, processed and analyzed remotely for performance degradation detection and faults diagnostics.
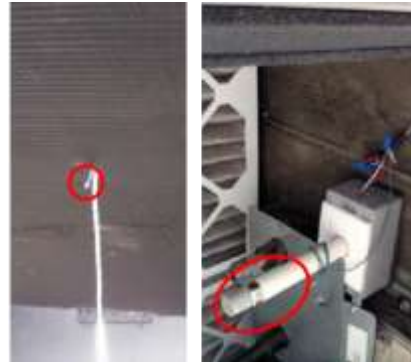
Contains no technical data subject to the EAR or the ITAR

a) Exterior Photo/Enclosure

b) WebCTRL Interface
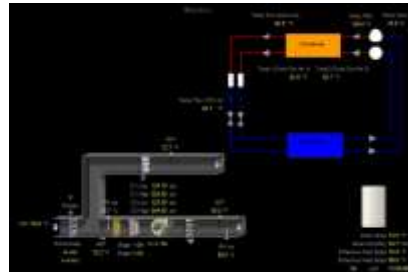

c) Thermistors along Refrigerant Loop

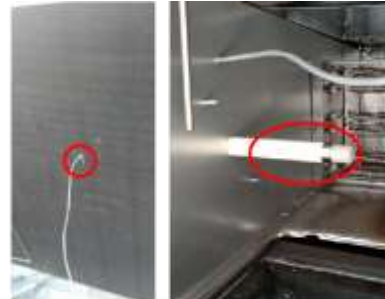d) Air Temp Probes & RH sensors

Figure 2.7 RTU-2 at 7-Eleven Store (801 Cape Coral pkwy, Cape Coral, FL)

a) Exterior Photo/Enclosure
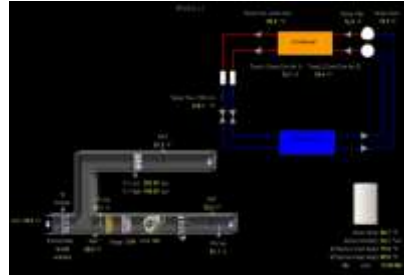

b) WebCTRL Interface

c) Thermistors along Refrigerant Loop   d) Air Temp Probes & RH sensors

Figure 2.8 RTU-1 at 7-Eleven Store (1548 Andalusia Blvd, Cape Coral, FL)

a) Exterior Photo/Enclosure   b) WebCTRL Interface

c) Thermistors along Refrigerant Loop   d) Air Temp Probes & RH sensors

Figure 2.9 RTU-2 at 7-Eleven Store (1548 Andalusia Blvd, Cape Coral, FL)

2.3 Test Matrix

Table 2.2 Test matrix of Field Demonstration

| Fault Sources	Fault Type	Detection and Diagnostics Approach
Injected Faults	• Condenser blockage	Recorded data analysis before after applying screen blockage on condenser
	• Evaporator blockage	Recorded data analysis before after applying screen blockage on evaporator
	• Condenser & evaporator blockage	Recorded data analysis before after applying screen blockage on evaporator & condenser
	• Compressor leakage	Recorded data analysis before after reducing refrigerant charge
Naturally Occurring Faults	• Condenser fouling • Evaporator fouling • Compressor leakage • Liquid line constrain • Refrigerant leakage	Historical data analysis and operation sanity check with developed virtual and additional physical sensor measurements.

As shown in Table 2.2, the testing matrix includes naturally occurring faults and faults manually injected during RTU operation. For the naturally occurring faults, RTU performance degradation could be caused

by single or multiple faults. Not only a single fault but also double faults will be injected simultaneously during the field tests. The planned injected faults include condenser blockage, evaporator blockage, and compressor leakage.

2.4 Commissioning and Data Retrieving

After the installation and WebCRTL interface upgrade, all sensors and additional data acquisition were commissioned. During the commissioning, a few abnormalities in both temperature and humidity measurement were found. UTRC, ALC, and Face Inc. worked together and fixed the majority of issues. Meanwhile the related historical field testing data were downloaded remotely and analyzed. Figures 2.10-2.13 show retrieved data from September 5, 2015 to September 9, 2015.
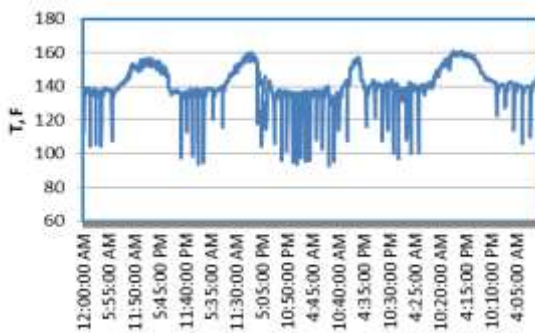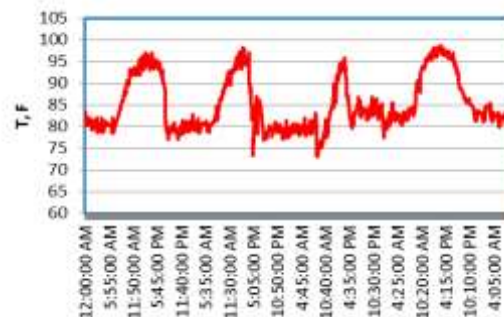
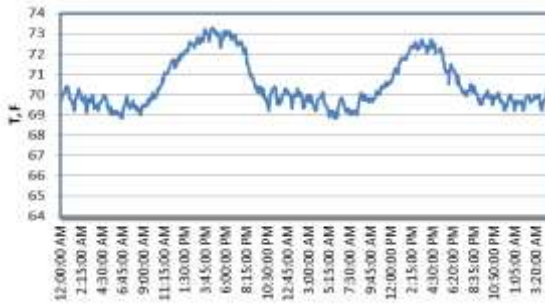a) Compressor Discharge Temperature   b) Compressor Suction Temperature
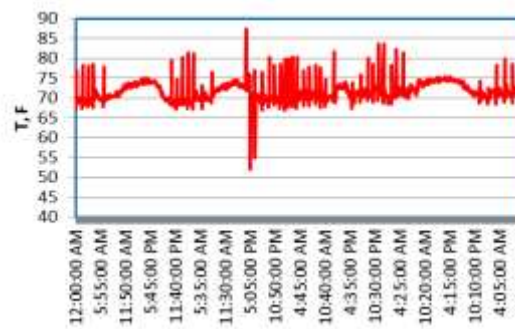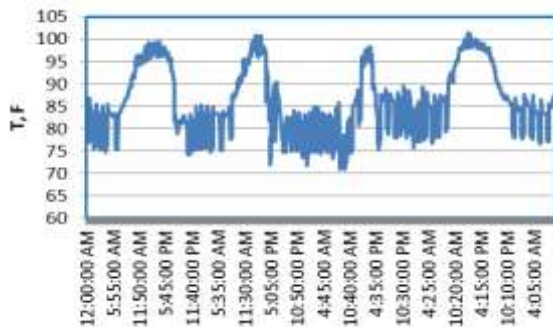
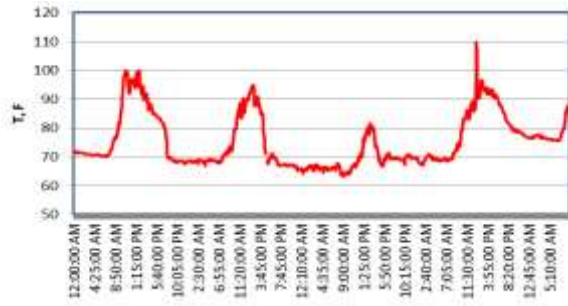c) Condenser Outlet Air Temperature   d) Condenser Refrigerant Outlet Temperature

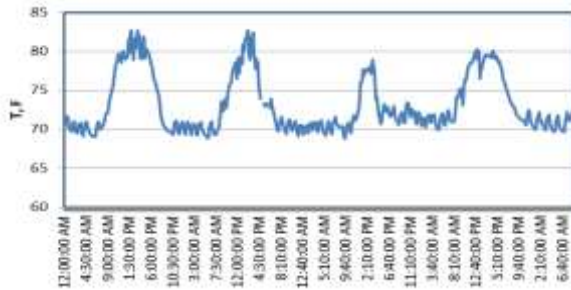Figure 2.10 RTU-1 at 7-Eleven Store (801 Cape Coral pkwy, Cape Coral, FL)

a) Zone Air Temperature

b) Condenser Outlet Air Temperature

c) Mixing Air Temperature

d) Mixing Air Relative Humidity

Figure 2.11 RTU-2 at 7-Eleven Store (801 Cape Coral pkwy, Cape Coral, FL)

a) Compressor Discharge Temperature
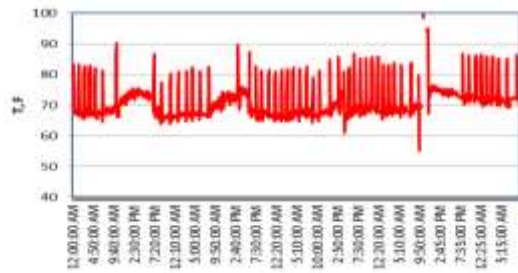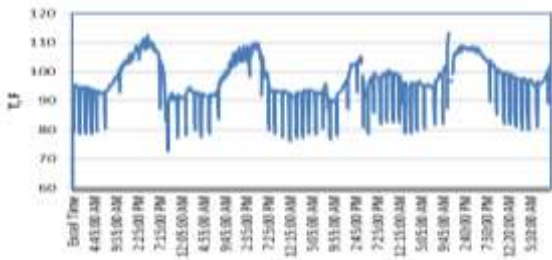
b) Compressor Suction Temperature

c) Condenser Outlet Air Temperature
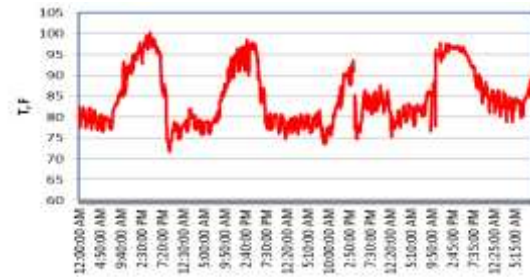
d) Condenser Refrigerant Outlet Temperature

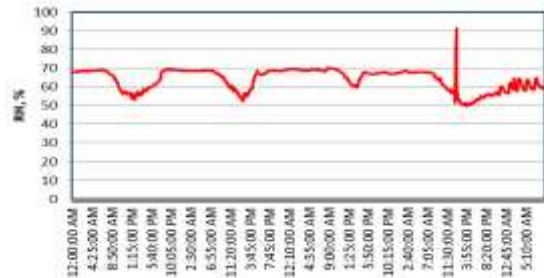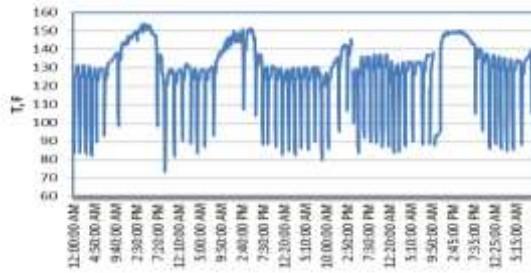Figure 2.12 RTU-1 at 7-Eleven Store (1548 Andalusia Blvd, Cape Coral, FL)
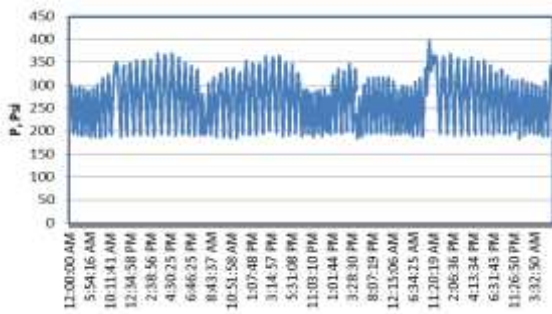
a) Compressor Discharge Pressure
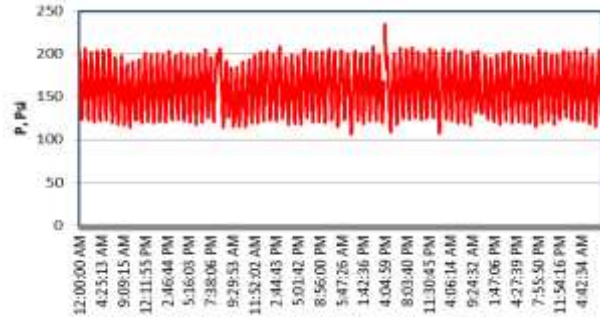
b) Compressor Suction Pressure
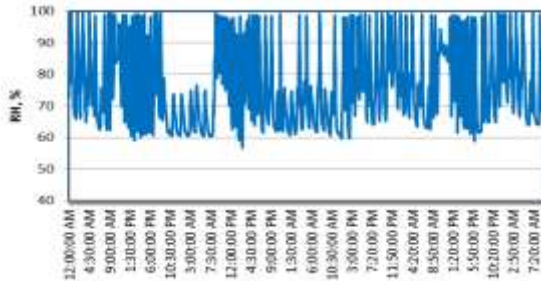
c) Supply Air Relative Humidity
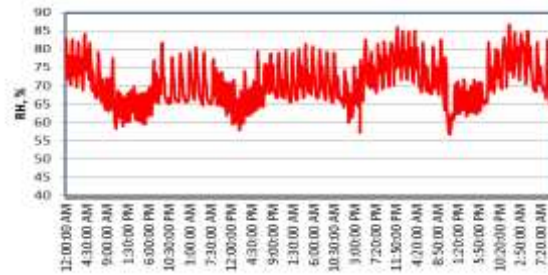
d) Mixing Air Relative Humidity

Figure 2.13 RTU-2 at 7-Eleven Store (1548 Andalusia Blvd, Cape Coral, FL)

3   RTU FDD Implementation

3.1 RTU Performance Diagnostics
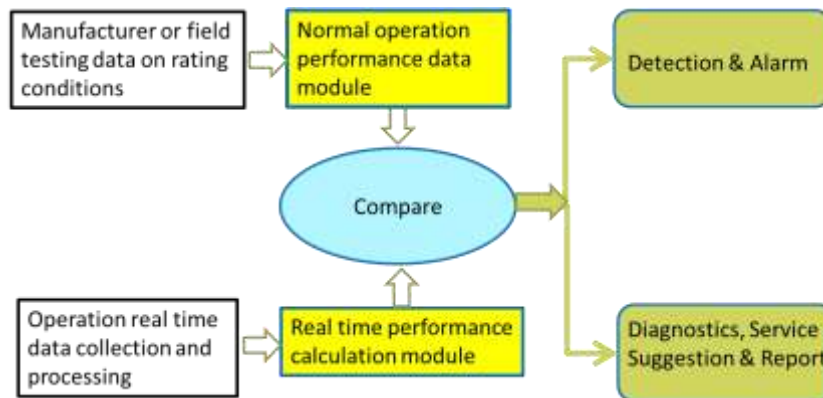
Figure 3.1 Overall Layout of AFDD Methodology Implementation

Contains no technical data subject to the EAR or the ITAR

Overall RTU performance diagnostics approach is shown in Figure 3.1. RTU operational performance is of greatest concern to end users because its degradation results in lower energy efficiency and therefore higher electricity bills. RTU performance degradation is assessed by comparing the real time RTU performance (cooling capacity and COP) with the expected performance under the same operation conditions without any fault, i.e.

$$\varepsilon_Q = 1 - \frac{Q}{Q_{ref}} \tag{3.1a}$$

$$\varepsilon_{COP} = 1 - \frac{COP}{COP_{ref}} \tag{3.1b}$$

RTU performance degradation is monitored real time and an alarm will be issued once either capacity or COP degradation exceeds a preset value (ε_{limit}, e.g. 10%)

$$\varepsilon_Q \text{ or } \varepsilon_{COP} > \varepsilon_{limit} \tag{3.2}$$

RTU real time performance is estimated as the flow chart shown in Figure 3.2. RTU expected performance is calculated by the reference model generated from the manufacturer's system models. It is described in the next section.
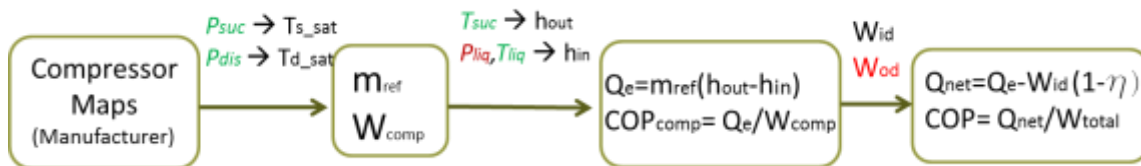
Figure 3.2 Real Time Performance Calculation Flow Chart

3.2 Referenced Model Development

The reference performance models for the RTUs in both 7-eleven stores are generated from the RTU system models provided by their manufacturer (Carrier). The 5-ton RTU (HCQ06) is a single R410A loop system while the 7.5 ton RTU (HCQ08) has two independent R410A loops.

Since the beginning of BP5, UTRC has been working very closely with Carrier, ALC, the 7-Eleven chain and facility managers on site selection, WebCRTL remote access, additional sensor installation and commissioning. Documentation on both 5 and 7.5 ton RTUs has been collected from Carrier. Figure 3.3 shows system configuration information needed for performance calculations. The 5-ton RTU is a single R410A loop system while the 7.5 ton RTU has two independent R410A loops.

Figure 3.4 shows the flow chart for generating reference models and calculating RTU expected performance under normal operation condition. The RTU reference model is an empirical curve fitting from multiple simulation results of the manufacturer system models. Variables in the curve fitting

process are outdoor ambient temperature (T_{amb}) and indoor dry and wet bulb temperatures (T_{id_db} & T_{id_wb}). The formulas for curve fitting are the following:

$$Q_{ref} = (a_0 + a_1 T_{amb} + a_2 T_{amb}^2 + a_3 T_{wb} + a_4 T_{wb}^2 + a_5 T_{db} + a_6 T_{db}^2 + a_7 T_{amb} T_{wb} + a_8 T_{amb} T_{db} + a_9 T_{wb} T_{db})(a_{10} + a_{11} T_{amb}) \qquad (2.10)$$

$$W_{net} = b_0 + b_1 T_{amb} + b_2 T_{amb}^2 + b_3 T_{wb} + b_4 T_{wb}^2 + b_5 T_{db} + b_6 T_{db}^2 + b_7 T_{amb} T_{wb} + b_8 T_{amb} T_{db} + b_9 T_{wb} T_{db}$$
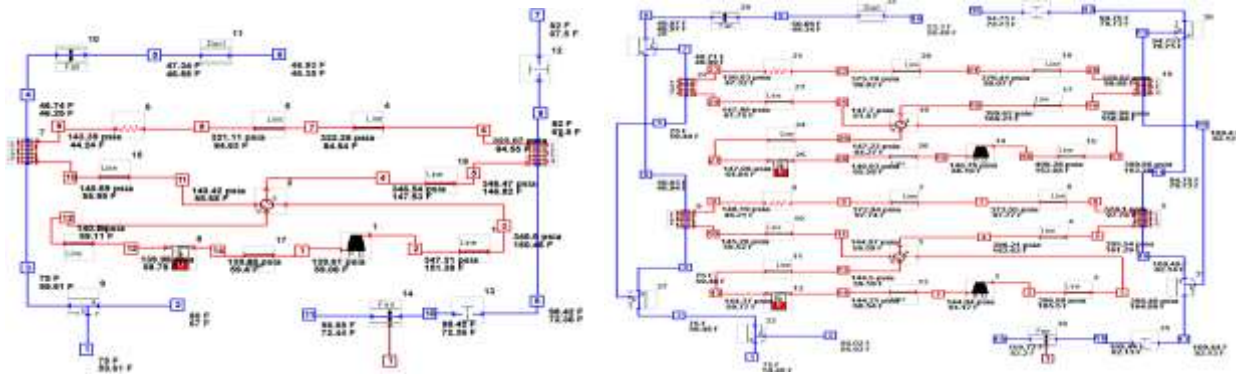
a) 5-ton Unit (HCQ06)   b) 7.5-ton Unit (HCQ08)

Figure 3.3 Carrier's RTU System Models
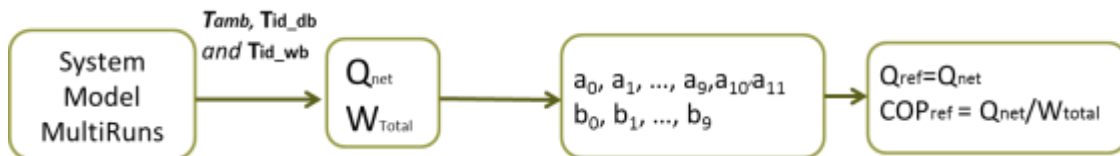
Figure 3.4 Flow Chart of Reference Model Generation

$$(2.11)$$

RTU expected COP is estimated by the following formula:

$$COP_{ref} = Q_{ref}/W_{net} \qquad (2.12)$$

Table 3.1 lists the values used for the system model parametric simulations. Based on the simulation results, the reference model coefficients for both cooling capacity and power are obtained by least squares regression.

Table 3.1 Values for Parametric Simulations

T_{OD}, F	T_{ID_DB}, F	RH_{ID_air}, %
70,75,80,85,90,95	68,70,72,74,76,78,80	50,55,60,65,70,75,80

3.3 AFDD Field Implementation

Overall AFDD implementation for field RTUs is shown in Figure 3.5. DAQ is integrated with RTU controller. Related RTU operation data are collected and displayed through ALC online platform WebCRTL. The UTRC developed data management system (middleware) retrieves data from WeCTRL platform and stores it in a data server. Executable FDD module analyzes the retrieved data and outputs results about RTU operation performance and possible faults.

Figure 3.5 Flowchart of Field AFDD Implementation

Current FDD module is developed by modifying the Python based FDD codes from Purdue University. Furthermore, an automatic online FDD is developed by integrating the data retrieving, analyzing and result outputs together. The application interfaces of the data acquisition platform and integration with the diagnostic algorithms are described in the following paragraphs.

The overall architecture of remote data access is shown in Figure 3.6. It builds on a data access layer, called the Data Management System (DMS), which maps WebCTRL historian data points to a local database to provide easy access to data from local machines using a simple application protocol interface (API).
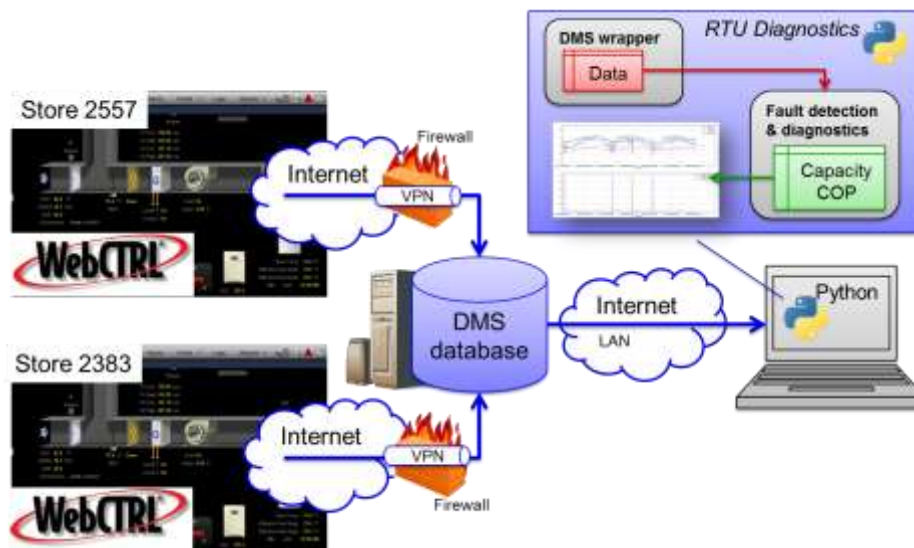
Figure 3.6 Architecture of remote data access

The Data Management System (DMS), developed by UTRC over the course of several previous projects, provides a common interface that standardizes the data access mechanism across various building systems to address the varying needs of industries that UTC operates in. It adopts the concept of data abstraction from the real data objects present in a data store (e.g. WebCTRL). This abstract data object has communication metadata associated with it that contains all the information on how to access the real data object (e.g.: ID of the data point, type of protocol to use, IP or endpoint of the service provider etc.).

WebCTRL is a software application that generates the values of data objects (variables) from sensors or controllers (that sample readings). This is the end application/protocol which the DMS engages with to abstract the data and collect the data values to its local database. WebCTRL historian application is the data store that stores values of data objects. WebCTRL historian preserve the history (or trend) of data objects. It provides an interface to allow other applications to access its data objects.

In the RTU diagnostics project, the DMS is utilized to communicate with WebCTRL by leveraging the capability of abstract data objects in hiding all the complexity and details of communications in the data access layer. RTU diagnostics application uses only the Data Management System interface to issue queries about the data. The DMS, in turn, is responsible to translate each query to appropriate abstract data object, map the abstract data object that to its real counterpart and to send the response back to the RTU diagnostics application in a predefined format. For seamless and continuous operation, the DMS collects the data values to its local database, as long as data queries are predefined. The particular use case for RTU diagnostics is interested in historic and trend data. Historic data retrieval is supported by the DMS. In this case, the DMS captures data from the WebCTRL historian by starting data access to

all the data points of interest from a starting time until the run time of the DMS catches up with the run time of data generation. Therefore, the data can be managed and stored by the DMS locally.

RTU diagnostics application interacts with the DMS by sending requests about data that is managed by the DMS. The RTU diagnostics application does not have to concern itself with how the actual communication with the data sources took place, i.e. the protocol in use, as this is handled by the DMS. The DMS is in charge of using appropriate protocol to initiate the communications to the WebCTRL. In this case, the internet protocol (IP) is used to interface with the WebCTRL historian data points, which reside behind a firewall. In fact, there are two separate servers of WebCTRL that hosts the data generated from two physical locations. Each server serves to a single location and is accessed separately by the DMS using a VPN tunnel over IP.

RTU diagnostics application and the DMS communicate over a local area network (LAN). Although physically the machine that hosts the DMS and the machine that hosts the RTU diagnostics application are not the same, they are behind the same firewall, which allows them to communicate without another VPN tunnel. The DMS allows multiple clients at a time. Therefore, it is conceivable to host DMS in any physical location and access the data from multiple RTU diagnostics applications within or outside the firewall.

RTU diagnostics application uses a DMS API (wrapper) to issue a data query to the DMS. This API is written in Python language to be able to interface easily with the RTU diagnostics algorithms. Once a data query is received by the DMS from RTU diagnostics application, DMS responds back with the data in a predefined format. The data received by the RTU diagnostics application is in the memory of the application and passed to the diagnostics algorithms of the application for further data processing. The data is also stored locally as a comma delimited file.

4   Field Demonstration

4.1 Overview
After installing additional sensors and commissioning the DAQ system, a series of field demonstrations have been performed successfully in spite of the challenges of RTU field operations including frequent on-offs, unusual environmental conditions and signal noises et al. Before any applications, the reference models were calibrated and validated. They are described in the following section.

4.2 Field Testing Data Analysis & Referenced Model Calibration
Based on the compressor map from the manufacturer, the actual refrigerant flow rate (m_{ref}) and compressor power (W_{comp}) can be calculated by the following formula:

$$m_{ref} = M_0 + M_1 T_{Ss} + M_2 T_{DS} + M_3 T_{ss}^2 + M_4 T_{ss} T_{DS} + M_5 T_{DS}^2 + M_6 T_{SS}^3 + M_7 T_{SS}^2 T_{DS} +$$
$$M_8 T_{SS} T_{DS}^2 + M_9 T_{DS}^3 \qquad (4.1)$$

$$W_{comp} = W_0 + W_1 T_{Ss} + W_2 T_{DS} + W_3 T_{ss}^2 + W_4 T_{ss} T_{DS} + W_5 T_{DS}^2 + W_6 T_{SS}^3 + W_7 T_{SS}^2 T_{DS} +$$
$$W_8 T_{SS} T_{DS}^2 + W_9 T_{DS}^3 \qquad (4.2)$$

Coefficients of the compressor maps were provided by Carrier. The 5-ton RTU (HCQ06) has a ZP49K5E-PFV_60_AC scroll compressor while the 7.5-ton RTU (HCQ08) has two ZP39K5E-TF5_60_AC compressors.

RTU net cooling capacity and COP are estimated as follows:

$$Q_{net} = m_{ref}(h_{e,out} - h_{e,in}) - W_{id}(1 - \eta) \qquad (4.3)$$

$$COP = \frac{Q_{net}}{W_{comp} + W_{od} + W_{id}} \qquad (4.4)$$

where $h_{e,out}$ and $h_{e,in}$ are refrigerant enthalpy at the inlet and outlet of the evaporator, w_{id} and w_{od} are the indoor and outdoor fan powers and h is the indoor fan efficiency.

The evaporator refrigerant inlet enthalpy is approximated as the enthalpy at the condenser outlet temperature and compressor discharge pressure. The evaporator refrigerant outlet enthalpy is used as the compressor inlet enthalpy. As both indoor and outdoor fans run at constant speed, their power and efficiency from the manufacturer's system model are adopted for the RTU real time performance estimation. Their values are listed in Table 4.1.

Table 4.1 Indoor and Outdoor Fan Power and Efficiency of RTUs

|	W_{id_fan}, W	η_{id_fan}, %	W_{od_fan}, W	η_{od_fan}, %
5.0 Ton RTU (HCQ06)	317	26.7	308	18.9
7.5 Ton RTU (HCQ08)	771	25.6	577	37.6

Field operation data for both sites from October 4, 2015 to October 11, 2015 were retrieved, processed and analyzed. Figures 4.1 and 4.2 show the details of the retrieved data of the 7.5-ton RTUs on both sites. Figure 4.1 shows the 1st stage compressor suction and discharge pressures, air mixing and supply temperatures, and the indoor and outdoor relative humidity measurements of the 7.5-ton RTU located at 7-Eleven store at 801 Cape Coral pkwy, Cape Coral, FL. The 7.5-ton RTU (RTU-1) has two independent circuits. Their operation logic depends on the cooling demands and outdoor temperature. During the daytime, both stages are usually turned on or the 1st stage is on while the 2nd stage may be on or off. During the night time, the 1st stage is turned on or off while the 2nd stage usually is off for most of the time. Figure 4.2 shows the 1st stage compressor suction and discharge pressures, air mixing and supply

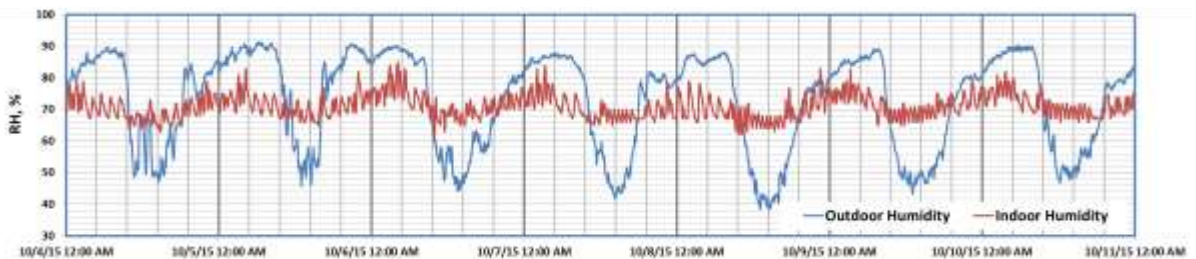temperatures, and the indoor and outdoor temperatures of 7.5-ton RTU located at 7-Eleven store at 1548 Andalusia Blvd, Cape Coral, FL. Its operation schedule is similar to the previous one.
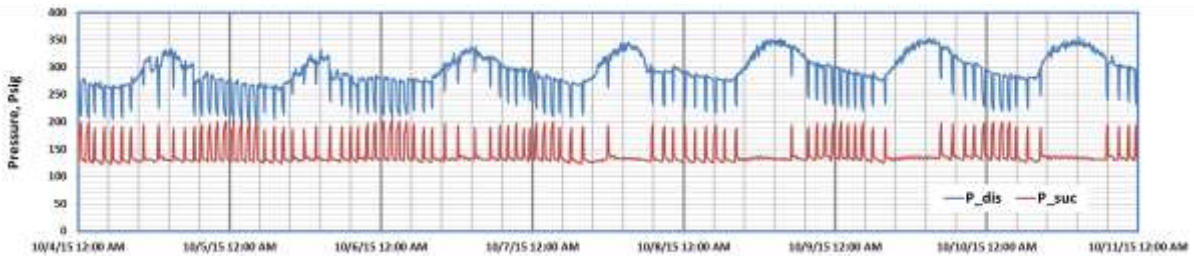
a) 1st Stage Compressor Discharge and Suction Pressure
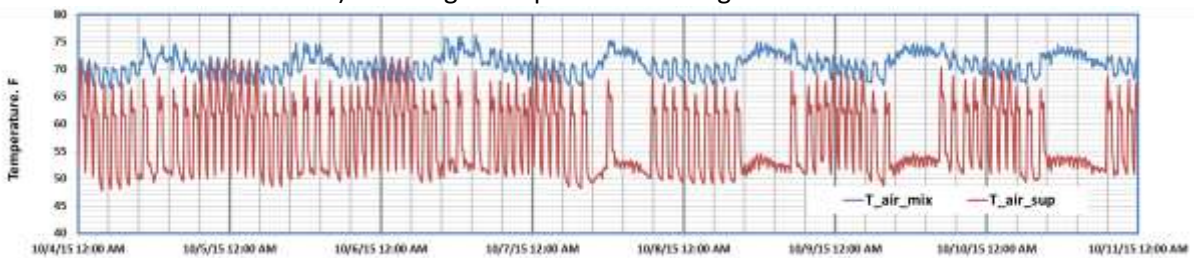
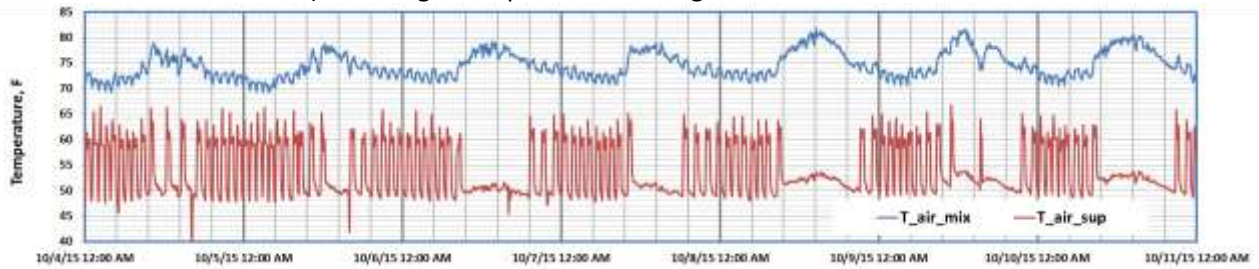b) Mixing Air and Supply Air Temperatures

c) Indoor and Outdoor Humidity

Figure 4.1 Field Data of RTU-1 at 7-Eleven Store (801 Cape Coral pkwy, Cape Coral, FL)
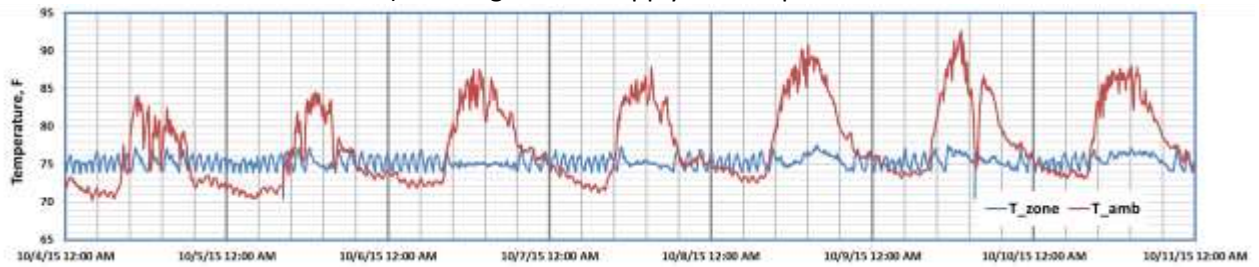
a) 1st Stage Compressor Discharge and Suction Pressure

b) Mixing Air and Supply Air Temperatures

C) Zone and Ambient Temperatures

Figure 4.2 Field Data of RTU-1 at 7-Eleven Store (1548 Andalusia Blvd, Cape Coral, FL)

The first three days of data were used to calibrate the reference models developed from the manufacturer system model.   After the calibration, the reference models were used for the RTU performance prediction under normal condition without any fault. The reference models include the RTU cooling capacity and power. RTU COP is calculated from the obtained cooling capacity and power. Figures 4.3 to 4.6 show the performance comparison of both 7.5-ton RTUs between the reference model predications and field measurements. The following formulae are utilized to show their differences or errors:

$$Error_Q = (Q_{net} - Q_{ref})/Q_{ref} \tag{4.5a}$$

$$Error_P = (P_{net} - P_{ref})/P_{ref} \tag{4.5b}$$

$$Error_{COP} = (COP - COP_{ref})/COP_{ref} \tag{4.5c}$$
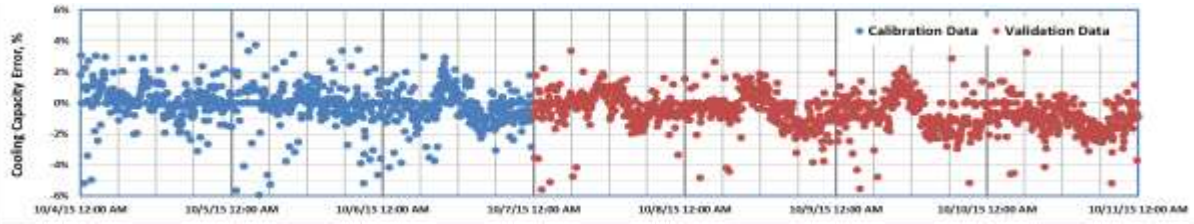
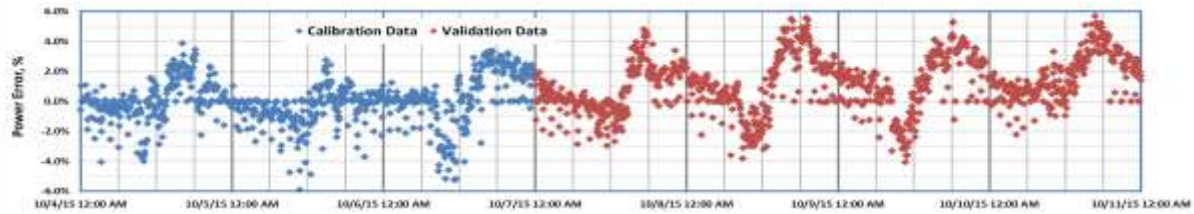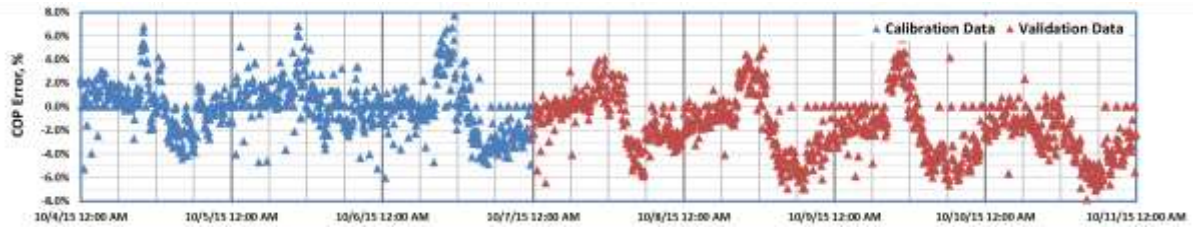a) Cooling Capacity Comparison

b) RTU Total Power Comparison

c) RTU COP Comparison

Figure 4.3 Results of RTU-1 at 7-Eleven Store (801 Cape Coral pkwy, Cape Coral, FL)
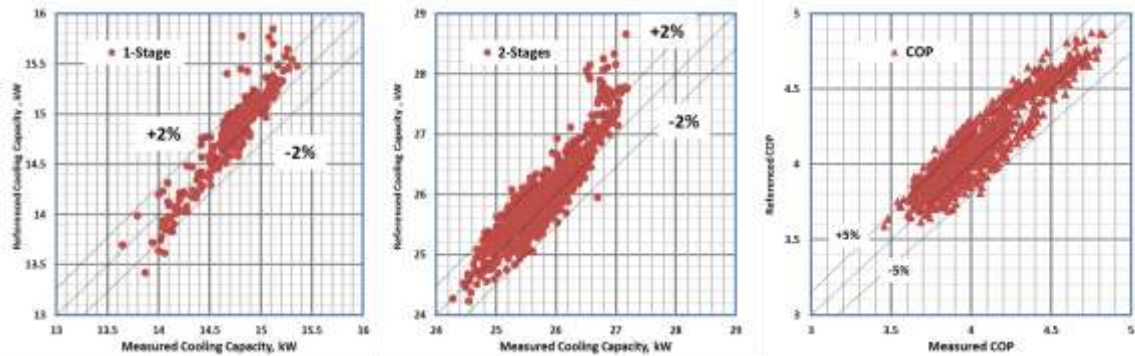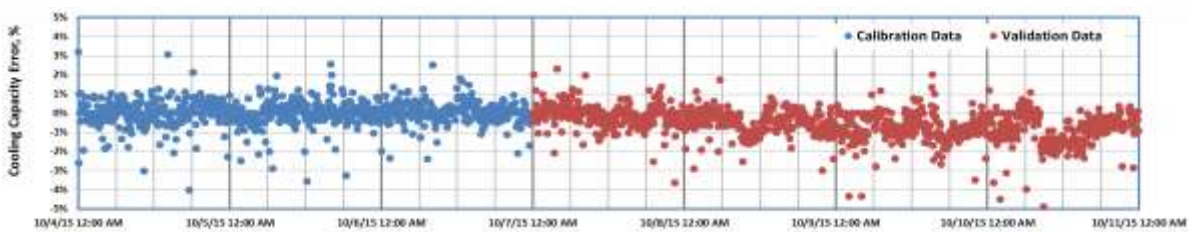

Figure 4.4 Performance Comparison of RTU-1 at 7-Eleven Store (801 Cape Coral pkwy, Cape Coral, FL)
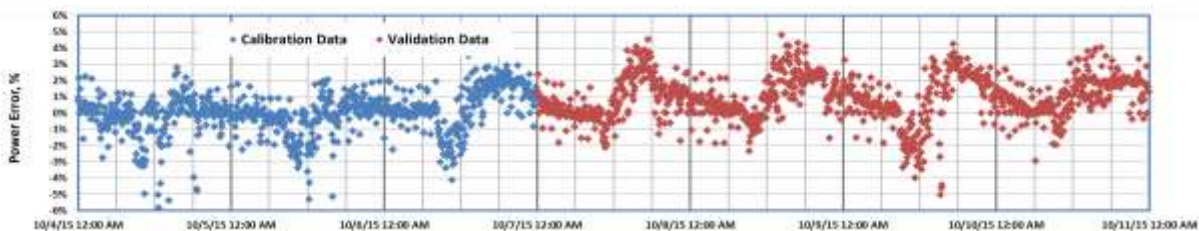
Figures 4.3 and 4.4 show the results of the 7.5-ton RTU (RTU-1) in 7-eleven store at 801 Cape Coral pkwy, Cape Coral, FL. The validation results show the differences between the field measurements and the reference models are within +2% to -4% of the cooling capacity, +5% to -3% of the total power and +4% to -6% of COP for the majority of the validation data points. The average errors for the four days are -0.64% (Oct. 7 -0.22%, Oct. 8 -0.52%, Oct. 9 -0.70%, Oct. 10 -1.10%) for the cooling capacity, -1.80% (Oct. 7 -0.87%, Oct. 8 -1.65%, Oct. 9 -1.80%, Oct. 10 -2.87%)   for the total power and 1.23% (Oct. 7 0.69%, Oct. 8 1.21%, Oct. 9 1.18%, Oct. 10 1.85%) for COP. Based on the validation results, it is concluded that the 7.5-ton RTU operated normally and no performance degradation was found during October 7 to October 11, 2015.

Figures 4.5 and 4.6 show the results of 7.5-ton RTU (RTU-1) in 7-eleven store at 1548 Andalusia Blvd, Cape Coral, FL. The differences between the field measurements and the reference models are within +1% to -3% of the cooling capacity, +4% to -2% of the total power and +3% to -5% of COP for the majority of the validation data points. The average errors for the total four days are -0.6% (Oct. 7 -0.11%, Oct. 8 -0.51%, Oct. 9 -0.82%, Oct. 10 -0.92%) for the cooling capacity, -1.52% (Oct. 7 -0.95%, Oct. 8 -1.57%, Oct. 9 -1.54%, Oct. 10 -2.00%)   for the total power and 0.96% (Oct. 7 0.86%, Oct. 8 1.08%, Oct. 9 0.76%, Oct. 10 1.11%) for COP. The validation results show the 7.5-ton RTU also operated normally and no performance degradation was found in the testing period.
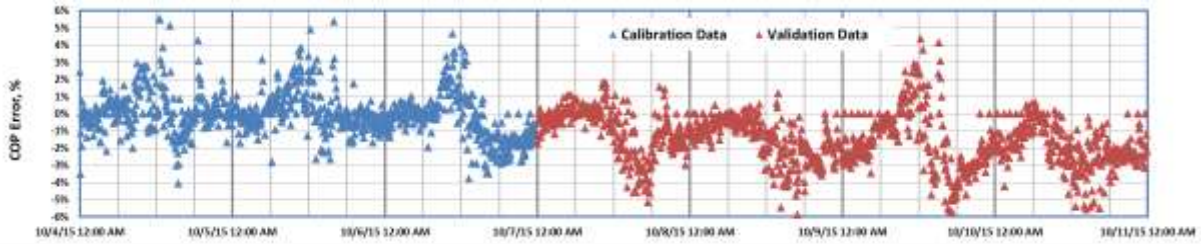

a) Cooling Capacity Comparison

b) RTU Total Power Comparison

CBEI REPORT

c) RTU COP Comparison

Figure 4.5 Results of RTU-1 at 7-Eleven Store (1548 Andalusia Blvd, Cape Coral, FL)
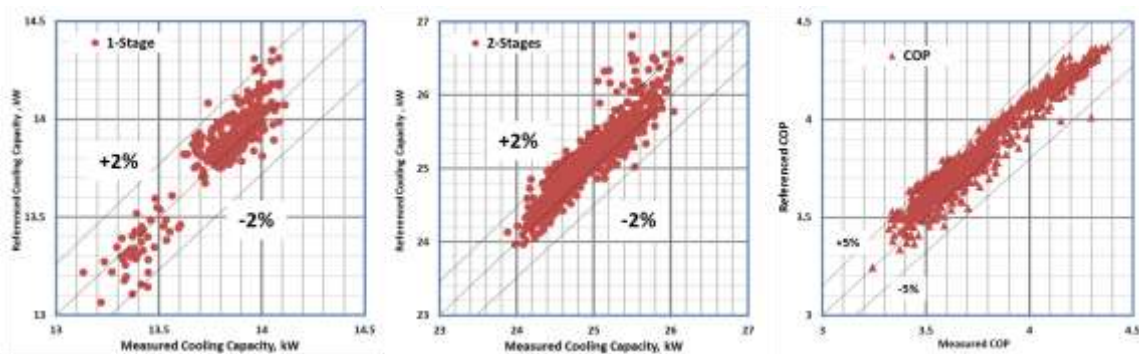
Figure 4.6 Performance Comparison of RTU-1 at 7-Eleven store (1548 Andalusia Blvd, Cape Coral, FL)

4.3 Field Testing under Fault Injection

Table 4.2 Fault Injection Matrix

Injection Fault	Injection Method & Level	Impacts
Condenser Blockage	• Cover condenser coil air inlet with a blanket • None, 1/4, 1/2 and ¾ of total area	• Compressor and fan power increment • Outdoor Air flow reduced
Evaporator Blockage	• Cover full evaporator section with blankets (A &B) • None, single layer of A, single layer of B, Double Layers of Bs	• Compressor and blower power changes • Indoor Air flow reduced
Compressor Bypassing	• Bypass a compressor with refrigerant charge device • None, 1.5 and 3 turns (full open) of the control valve	• Compressor power increment
Evaporator and condenser Blockage	• Cover condenser filter with 1/4 size cardboards • None, 1/4, and 1/2 (diagonal position) of total area	• Compressor and blower power increment • Indoor & outdoor air flow reduced

| a) Condenser Blockage | b) Evaporator Blockage | c) Compressor Bypass | d) Cond. & Evap. Blockage |

Figure 4.7 Field Fault Injection Implementation Cases

After the calibration and validation, RTUs in both sites have been under monitoring and data collection. However, almost no naturally occurred degradation and fault have been detected. Hence, a series of fault injection field tests have been carried out during March 31- April 1, 2016. The injection faults are condenser blockage, evaporator blockage and compressor bypassing. Table 4.2 lists the fault injection testing matrix. In addition to a single fault injection, multiple simultaneous faults injection also has been tested. Figure 4.7 shows all four fault injection implementation cases. The field demonstration results are shown in Figures 4.8 and 4.9.
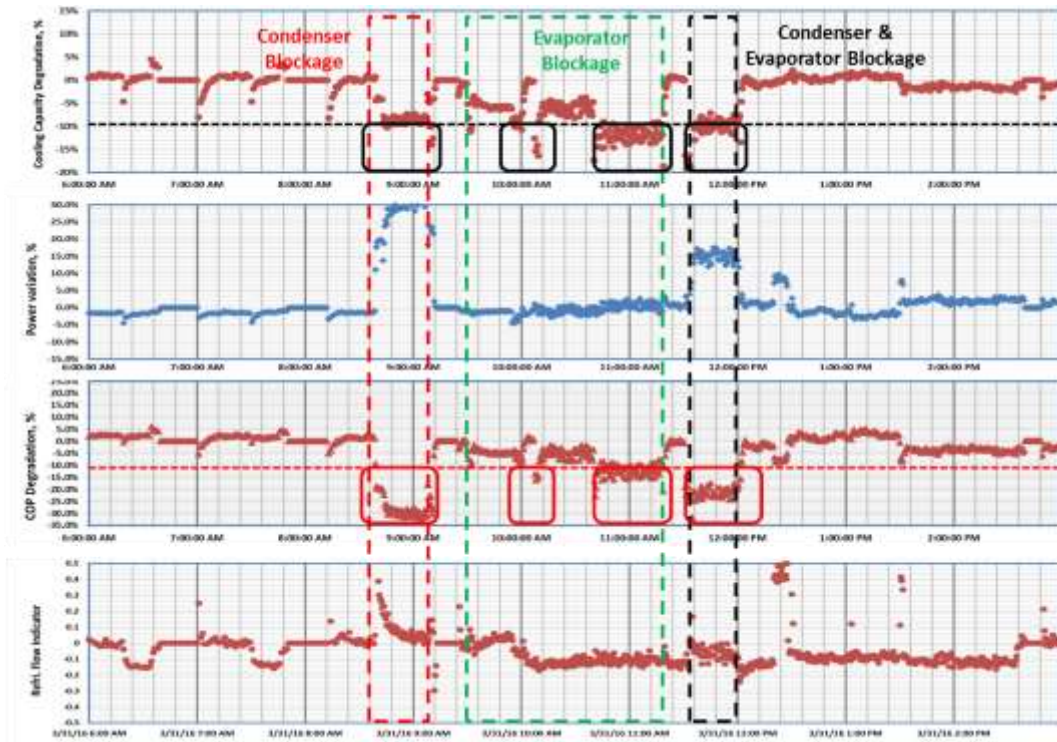
Figure 4.8 Results of Fault Inject Test (801 Cape Coral pkwy, Cape Coral, FL)

Figure 4.8 shows performance variations of the 7.5 ton RTU at 801 Cape Coral Pkwy under different fault injections. Under the condenser blockage RTU cooling capacity decreases, RTU total power increases significantly, and consequently RTU COP drops a lot. As shown in Figure 4.8, the cooling capacity drops about 10%, power increases at 25-30% and COP decreases at 30-35% under 75% area covered with a blanket. It is detectible if the threshold is set at 10% capacity or COP degradation. Under the evaporator blockage, RTU total power is nearly unchanged while the cooling capacity and COP decrease. Both cooling capacity and COP decrease at 6-9% and 10-15% under 35% and 50% evaporator blockage respectively. It can be detected and alarmed over 10% degradation. RTU performance degrades rapidly under simultaneous condenser and evaporator blockage. RTU cooling capacity decreases at 9-12%, total power increases 15% and COP goes down by 20-25% under 50% condenser area blockage and 35% evaporator blockage.
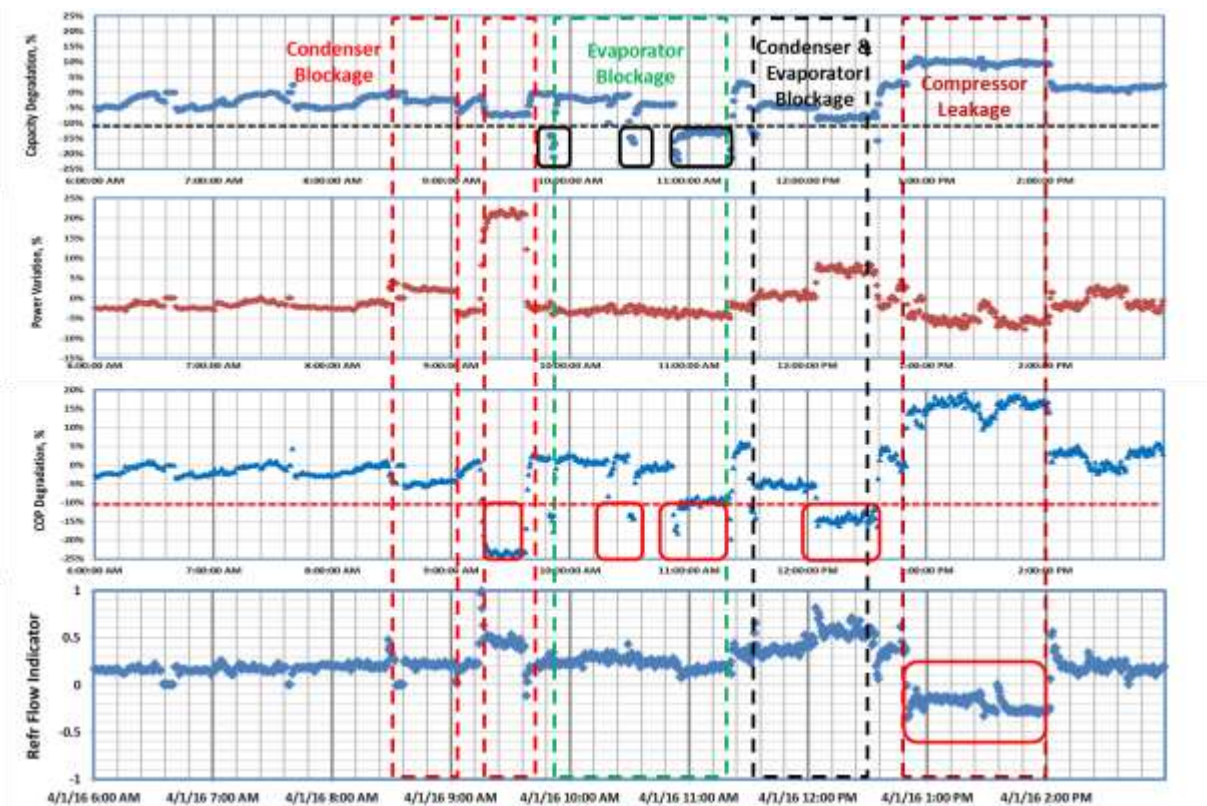

Figure 4.9 Results of Fault Inject Test (1548 Andalusia Blvd, Cape Coral, FL)

Figure 4.9 shows performance degradation detection of 7.5 ton RTU at 1548 Andalusia Blvd under fault injections. Under 50% condenser area blockage RTU cooling capacity slightly decreases while total power increases about 3-4% and COP decreases at 5%. When the condenser blockage increases to 75%,

the cooling capacity decreases at 6-7% while the total power jumps by 20%. Consequently, COP drops by 23-25%. Under the evaporator blockage, the total power very slightly decreases and the cooling capacity decreases around 5% and 15% at 35% and 50% evaporator blockage respectively. Under a simultaneous 50% condenser and 35% evaporator blockage, the cooling capacity decreases 6-8% and total power increases 6-8%. Consequently, the COP decreases around 15%. A compressor leakage is injected through bypassing a portion of the refrigerant flow from the discharge port to the suction port of the compressor. As shown in Figure 4.9, the cooling capacity calculated by the virtual refrigerant flow rate from the compressor map increases. However, the real refrigerant flow rate is lower than the virtual flow rate because of the compressor bypassing. Hence, the virtual refrigerant flow rate is inappropriate when there exists a compressor fault. A refrigerant flow indicator is developed by analyzing the compressor energy balance. The compressor flow indicator shows a significant flow deviation under the compressor bypassing. It is detectible for the injected compressor leakage. However, more study is recommended for understanding the compressor leakage behavior.

4.4 Results of AFDD Demonstration

As the injected faults are very limited during the field demonstration, it is not possible to draw conclusions about the statistical probabilities of the field fault detection rates. However, RTU fault detection rate statistics obtained from previous laboratory demonstration in UTRC can be utilized for analyzing current field demonstration results. Figures 4.10 and 4.11 show the detection accuracy statistical profiles of RTU performance degradation of 10% cooling capacity and COP. The false alarm rate will be less than 1% if the degradations of the cooling capacity and COP are more than 2.0% and 5.0% respectively. The fault detection confidence is more than 90% when the alarms are issued after the degradations of cooling capacity and COP reach 13.0% and 13.3% respectively.
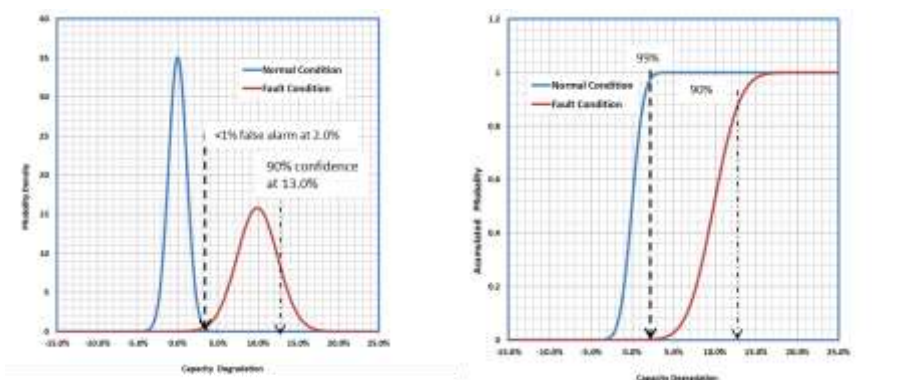

Figure 4.10 Accuracies of RTU Cooling Capacity Degradation Diagnostics
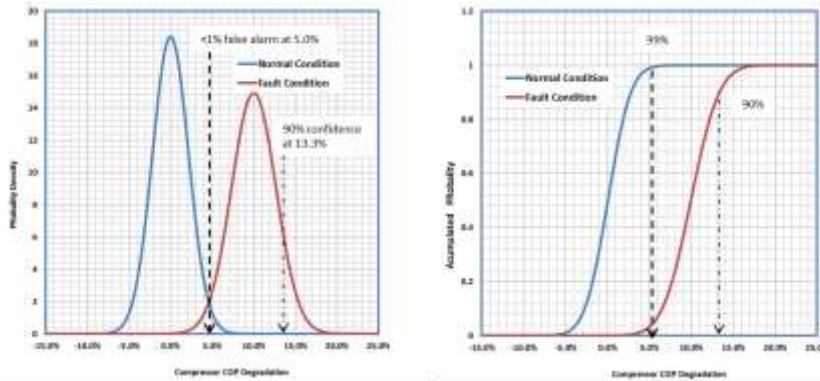
Figure 4.11 Accuracies of RTU Compressor COP Degradation Diagnostics

The AFDD field implementation described in Section 3.3 is applied for both 7.5-ton RTUs at the 7-eleven sites in Florida. The results are shown in Figures 4.12 and 4.13. Figure 4.12 shows the results of AFDD implementation on 7.5 ton RTU at 801 Cape Coral pkwy during February 25 to April 6, 2016. The only faults detected are the faults injected during March 31, 2016. The detailed results for March 31 show the RTU performance variations and the issued alarms during the fault injections. The detected faults include the condenser blockage, evaporator blockage, and simultaneous condenser and evaporator blockage. The confidence of 10% performance degradation is over 90% by setting the performance degradation limits at 13% for a fault alarm. No false alarm is issued during this period.

Figure 4.12 Results of AFDD Demo on 1st 7.5 ton RTU (801 Cape Coral pkwy, Cape Coral, FL)

Figure 4.13 Results of AFDD Demo on 2nd 7.5 ton RTU (1548 Andalusia Blvd, Cape Coral, FL)

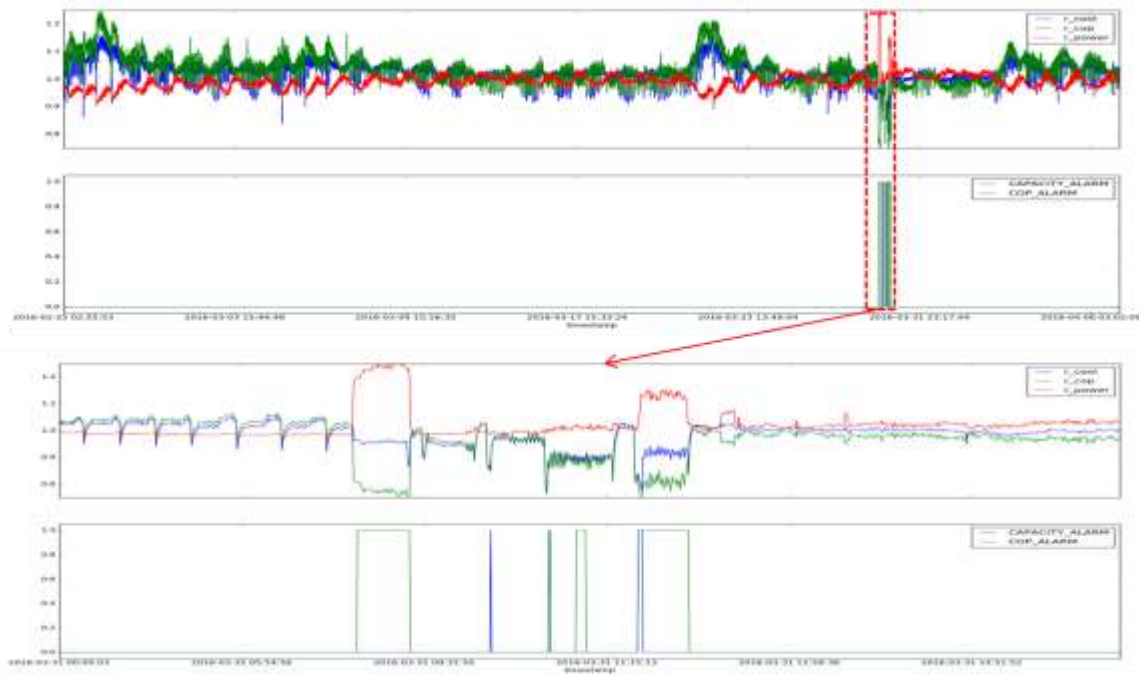Figure 4.13 shows the screening results of AFDD implementation on 7.5 ton RTU at 1548 Andalusia Blvd. during January 1 to April 6, 2016. The only faults detected are the faults injected during April 1, 2016. The detailed results during April 1 (shown in Figure 4.13) confirm the injected faults including the condenser blockage, evaporator blockage, and simultaneous condenser and evaporator blockage. As the RTU performance degradation limits (including cooling capacity and COP) are set at 13% for issuing a fault alarm, the confidence of 10% performance degradation is over 90%. No false alarm has been issued during this period too. Although it is not possible to claim the false alarm rate is 0% because of the limited fault data, from the statistics of the lab testing data the false alarm rate of the AFDD field demo on both RTUs should be much less than 1%.

4.5 Naturally Occurred Fault Detection

There is no naturally occurred performance degradation alarm issued from the AFDD field implementation for both 7.5-ton RTUs in Florida. However, the analyses of the detailed field data show the refrigerant leakage might occur on the 7.5 ton RTU at 1548 Andalusia Blvd. Figure 4.14 shows its cooling capacity variations between the beginning week of October, 2015 and the ending week of March 2016. The cooling capacity data from March show RTU cooling capacity decreases at around 3% in average by comparing with the referenced model calibrated in last October. However, this trend may not be enough to make a refrigerant leakage call. The refrigerant subcooling at the condenser outlet is checked for further evidence.
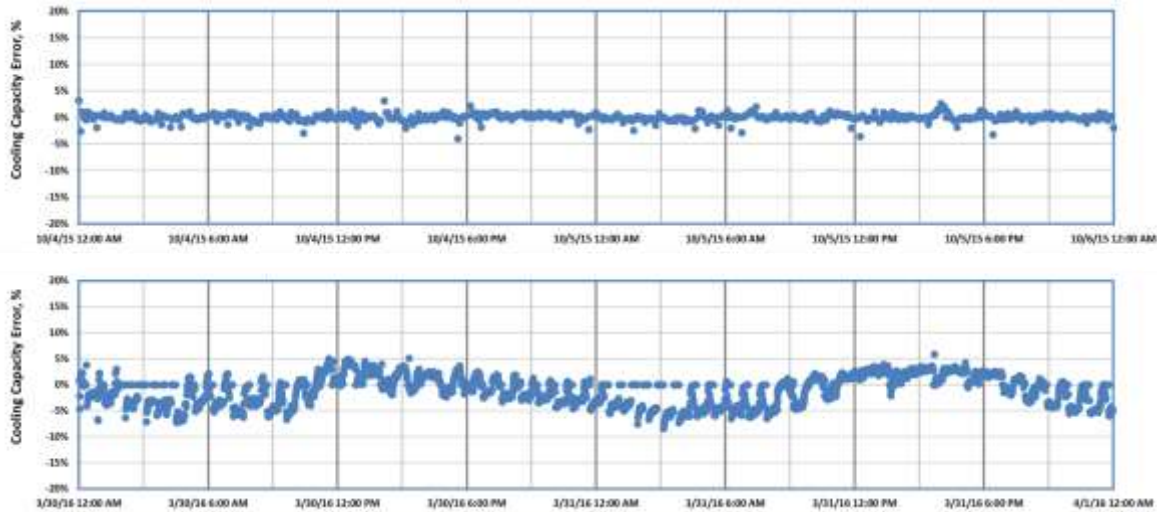
Figure 4.14 7.5-ton RTU Performance Variation Over time (1548 Andalusia Blvd, Cape Coral, FL)

Figure 4.15 shows the subcooling variations over time for this RTU including the outdoor temperature profiles for reference. Under the similar outdoor temperature profiles, the refrigerant subcoolings at the condenser outlet are significantly reduced from average 19 F to average 13 F. This significant subcooling reduction confirms the refrigerant leakage occurring over time for this RTU. This naturally occurred fault has been detected for this RTU.

Figure 4.15 7.5-ton RTU Condenser Outlet Subcooling Variation Overtime
(1548 Andalusia Blvd, Cape Coral, FL)

The detailed data analyses on the 7.5-ton RTU at 801 Cape Coral pkwy have not shown an obvious cooling capacity and subcooling reduction trends overtime. Hence, it is concluded that no refrigerant leakage detected for this RTU.

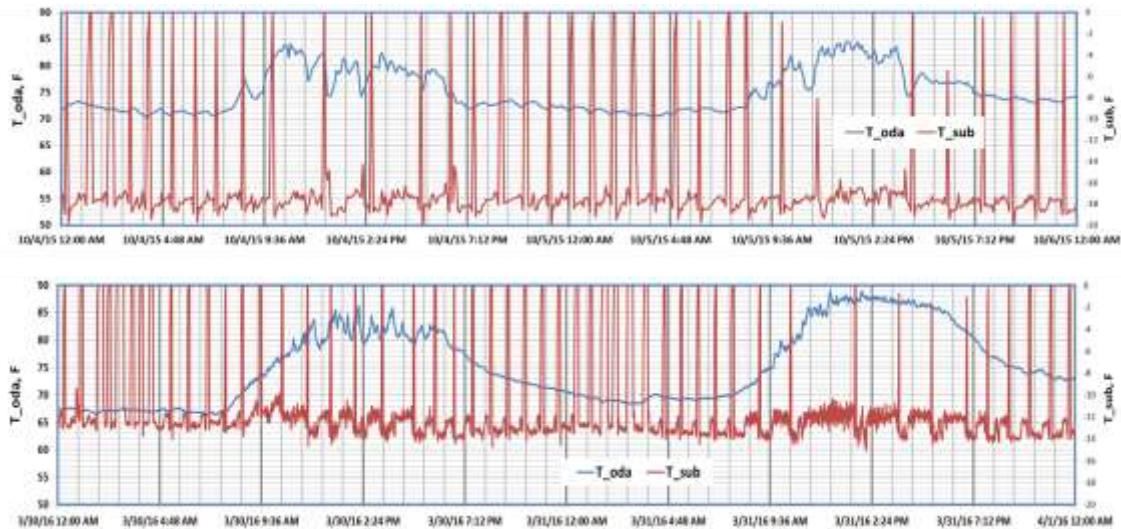# 5 Economic Assessment

The detailed assessment of payback period based on expected energy and maintenance cost savings was presented in BP4 final report [1]. The summary chart from that report is shown on Figure 5.1.
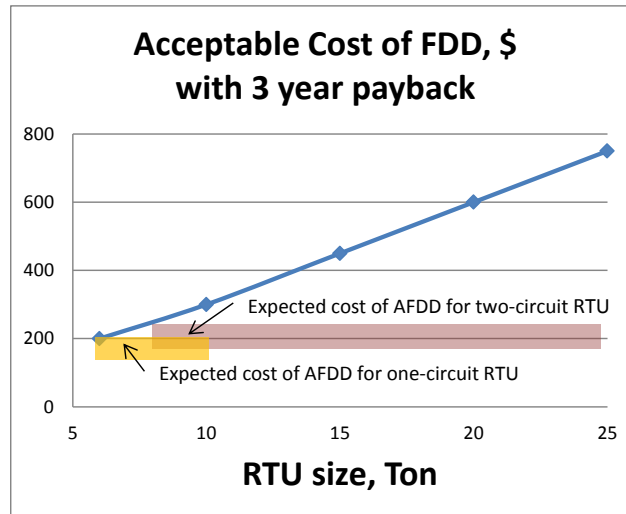

Figure 5.1 Acceptable and expected cost of FDD for different RTU size

The cost of installation for the current field demonstrations consists of the cost of the required sensors, their connection to the RTU controller and the cost of the mapping procedure and WebCTRL interface update. The required sensors are listed in Table 2.2. The cost of sensors, power supplies and expander boards for all four RTUs are listed in Table 2.3; for one RTU the cost was $1750. The cost of mapping and WebCTRL interface update for one RTU is $1108. So the total field installation cost per RTU is $2858. At this level of cost the retrofit solution is unrealistic in the cost sensitive RTU market. The cost reduction for can be achieved through factory installed solution as well as through standardization of the retrofit solution.

In the future state the installation for on-board embedded AFDD solution will be done in the factory environment and the sensors will be connected directly to the RTU controller with an additional I/O board. For similar units the costs of typical mass produced sensors are shown in Table 5.1. The sensor costs are taken from [9]. The additional cost of expected modifications to the I/O board is also included. The cost of full AFDD for one-circuit RTUs is estimated to be $200. This is based on additional hardware costs of about $135 (five additional temperature sensors ($25), two relative humidity sensors ($30), and an additional I/O board hardware ($80)) and installation labor costs of about $65. For two-circuit RTUs, another five temperature sensors are required ($25), and about ~$90 installation or total cost of $250. See table 2.1 for details of required sensors.

For RTU performance degradation detection option, which is the focus of initial commercialization path the number of required additional sensors is reduced only to three temperature sensors (see table 2.1)

CBEI REPORT

leading to total of $145 ($15 sensor cost, $80 I/O board hardware and $50 installation cost) for one-circuit and $175 ($30 sensor cost, $80 I/O board hardware and $65 installation cost).

Table 5.1 Typical hardware costs

Sensor	Cost($)
Physical sensor	
Relative Humidity	~$15
Refrigerant Temperature	~$5
Air Temperature	~$5
Refrigerant Pressure	~$20
Additional I/O board	~$80

During the seven month observation period (from October 2015 to April 2016), the major fault that was observed on four RTUs was the refrigerant leakage in one of the 7.5 ton RTUs leading to about 3% capacity reduction as described in section 4.5. This incident suggests a possibility of rather high frequency or prevalence of refrigerant leak faults in the systems with additional pressure sensors. Unfortunately the collected information due to its limited nature is statistically insufficient to make any meaningful general conclusions about frequency, type, and severity of typical faults. A study involving large numbers of RTUs is needed and should be undertaken as a continuation of this work.

6   Conclusions

The field demonstrations performed by the team within Project 2.2 present a significant step towards commercialization of AFDD technology for RTUs.
The project team has achieved the following accomplishments:

- Installed required instrumentation and remote monitoring system at two field sites
- Developed, calibrated and validated referenced models for AFDD
- Demonstrated performance degradation caused by different injected faults
- Developed online field data retrieving and system operation monitoring method
- Demonstrated online AFDD through WebCTRL platform and DMS middleware
- Achieved 90% confidence on 10% performance degradation detections with no false alarm during up to 3-month monitoring periods
- Performed economic assessment of AFFD solution

For commercialization of embeddable solutions, it is critical to involve commercialization partners in the development as early as possible.

The project team approached an RTU OEM (Carrier), a provider of building automation systems (ALC) and a National Account customer (7-Eleven) and secured their support for field demonstration of RTU

AFDD developed in BP4 [1]. The National Account customer 7-Eleven has expressed a strong interest in AFDD for RTUs and provided the demonstration sites.

The first commercial application for AFDD on RTUs is expected to be as a cost-effective embedded solution using the controller on new high tier units (Daikin, Carrier, etc.) [1]. Once a standard is established on lower tier units and the cost is reduced, market acceptance will increase. With this in mind, the demonstration in BP5 is being perfomed on state-of-the-art standard RTUs. AFDD performance results will be applicable to both high and low tier RTUs.

AFDD products could also be deployed as a standardized aftermarket service solution for the existing RTU installed-base (the benefit of AFDD will likely be higher on older RTUs).

Further systematic study of prevalence of typical faults in field conditions involving large numbers of RTUs is needed to strengthen AFDD value proposition.

7   References

[1] M. Gorbounov, J. Wang, H. Reeve, S. Yuan, A. Hjortland and J. Braun, "Project 2.2 – Fault Detection and Diagnostics (FDD) Final Report," Consortium for Building Energy Efficiency, 2015.

[2] H. Li and J. E. Braun, "A Methodology for Diagnosing Multiple Simultaneous Faults in Vapor-Compression Air Conditioners," *HVAC&R Research,* vol. 13, no. 2, pp. 369-395, 2007.

[3] W. Kim, Fault detection and diagnosis for air conditioners and heat pumps based on virtual sensors, West Lafayette, Indiana: Thesis (PhD) - Purdue University, 2013.

[4] M. S. Breuker and J. E. Braun, "Common faults and their impacts for rooftop air," *HVAC&R Research,* vol. 4, no. 3, pp. 303-318, 1998.

[5] D. P. Yuill and J. E. and Braun, "Evaluating the performance of fault detection and diagnostics protocols applied to air-cooled unitary air-conditioning equipment," *HVAC&R Research,* vol. 19, no. 1, pp. 882-891, 2013.

[6] D. P. Yuill, H. Cheung and J. E. and Braun, "Evaluating Fault Detection and Diagnostics Tools with Simulations of Multiple," in *International Refrigeration and Air Conditioning Conference*, 2014.

[7] K. W. Heinemeier, "Rooftop Fault Detection and Diagnostics: Technology and Market Review, Energy and Demand Savings Estimates," PIER, 2012.

[8] J. E. Braun and M. Gorbounov, "Workshop on FDD for RTUs, Milestone Report M2.2.c," CBEI, 2014.

[9] TIAX, "Energy Impact of Commercial Building Controls and Performance Diagnostics," TIAX, 2005.